NACA

RESEARCH MEMORANDUM

LARGE-SCALE FLIGHT MEASUREMENTS OF ZERO-LIFT DRAG AT

MACH NUMBERS FROM 0.90 TO 1.95 OF AN ARROW WING

IN COMBINATION WITH A SMALL BODY

By Warren Gillespie, Jr. and Richard G. Arbic

Langley Aeronautical Laboratory
Langley Field, Va.

NATIONAL ADVISORY COMMITTEE
FOR AERONAUTICS
WASHINGTON
January 12, 1951

319.98/13
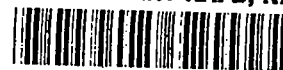
NATIONAL ADVISORY COMMITTEE FOR AERONAUTICS

RESEARCH MEMORANDUM

LARGE-SCALE FLIGHT MEASUREMENTS OF ZERO-LIFT DRAG AT

MACH NUMBERS FROM 0.90 TO 1.95 OF AN ARROW WING

IN COMBINATION WITH A SMALL BODY

By Warren Gillespie, Jr. and Richard G. Arbic

SUMMARY

A flight investigation was made at high subsonic, transonic, and supersonic speeds and at high Reynolds numbers to determine the zero-lift drag of an arrow wing-body combination and of the body without the wing. The wing had $67\frac{1}{2}^{O}$ leading-edge sweep, 15° trailing-edge sweep, and modified NACA 0004 sections. The body-wing area ratio was 0.0127.

The force-break Mach number of the wing-body combination was 0.98. A maximum drag coefficient of 0.0125 occurred at Mach number 1.03. The drag coefficient decreased from the maximum value almost linearly to a value of 0.0096 at Mach number 1.95.

INTRODUCTION

The Langley Pilotless Aircraft Research Division is investigating the aerodynamic characteristics of wing-body configurations suitable for supersonic flight through the use of rocket-propelled models. Continuous data are obtained from high subsonic to supersonic speeds at high Reynolds numbers.

This paper presents zero-lift drag data for an arrow wing-body combination and the body alone. The Mach number range was 0.90 to 1.95. Reynolds number, based on the wing mean aerodynamic chord of 2.31 feet, varied from 8.5×10^6 to 29.0×10^6.

SYMBOLS

C_D drag coefficient (Drag/qS)

C_N normal-force coefficient (Normal force/qS)

q   dynamic pressure, pounds per square foot

S   wing plan-form area (including area within body)

M   Mach number

R   Reynolds number

MODELS AND TESTS

The body and wing profile coordinates and the general arrangement of the two test configurations are presented in table I and figure 1, respectively. Photographs of the models and model-booster combinations are shown as figures 2 and 3, respectively. The body had a fineness ratio of 15.6. The frontal area of the body was 1.27 percent of the total wing area which was 5.61 square feet. The arrow wing had $67\frac{1}{2}^{\circ}$ leading-edge sweep, 15° trailing-edge sweep and modified NACA 0004 airfoil sections in the streamwise direction. The vertical tail of each model had 0° sweep at the 50-percent-chord line and a taper ratio of 0.23. Horizontal fins were used on the wingless model for stability.

The models were of composite wood-metal construction. The winged model was instrumented with a two-channel telemeter incorporating two accelerometers. The accelerometers were mounted to measure normal and longitudinal forces. The wingless model carried no instrumentation.

Figure 3 shows the models and external boosters in the launching position. An ABL Deacon rocket motor was used to propel the winged model. This rocket motor delivers approximately 6200 pounds thrust for 3.2 seconds. A smaller 5-inch HVAR rocket motor served to boost the wingless model.

Velocity was obtained from the CW Doppler radar and by integration of the data from the longitudinal accelerometer. Drag was obtained directly from the longitudinal accelerometer data and by differentiation of the Doppler determined velocity-time curve. Normal force was obtained from the normal accelerometer. Trajectory and atmospheric data were obtained from the radar tracking unit and by radiosonde observations, respectively.

The accuracy of the results is estimated to be:

Mach number . . . . ±0.010
C_D at Mach number 0.90 . . . . ±0.0010
C_D at Mach number 1.90 . . . . ±0.0005
C_N at Mach number 0.90 . . . . ±0.016
C_N at Mach number 1.90 . . . . ±0.002

RESULTS AND DISCUSSION

Curves of drag coefficient, Reynolds number, and normal-force
coefficient against Mach number are presented in figure 4(a) for the
wing-body combination. It is seen from the curve of normal-force coef-
ficient against Mach number that the drag data were obtained near the
zero-lift trim condition. The curve of drag coefficient against Mach
number of figure 4(a) shows that this configuration has a low supersonic
drag coefficient. From a peak value of 0.0125 at Mach number 1.03, the
drag coefficient decreased almost linearly to a value of 0.0096 at Mach
number 1.95. The force-break occurred at Mach number 0.98. The drag
coefficient of the model without the wing is shown in figure 4(b). The
drag of the two horizontal fins has been subtracted. The drag of these
fins was determined from tests in which four of these fins were mounted
as wings on a fin-stabilized body for which basic drag values were known.
The wing with interference drag, obtained by subtracting the corrected
drag of the wingless model from the drag of the wing-body combination, is
also shown in figure 4(b). The wing with interference drag was approxi-
mately 70 percent of the drag of the wing-body combination.

The drag coefficient of the wing-body combination tested is compared
in figure 5 with minimum drag coefficients of two similar configurations
at high values of Reynolds number ($R \geq 5 \times 10^6$). The model of refer-
ence 1, which had a body of fineness ratio 10, body-wing area ratio 0.0306,
and a 60° delta wing with NACA 65A003 airfoil sections, had a lower sub-
sonic drag coefficient than the model of the present test. At supersonic
Mach numbers, this large delta-wing model of reference 1 and the arrow
wing-body combination of the present test have very nearly equal values
of minimum drag coefficient. The 63.43° delta-wing model of reference 2
with 5-percent-thick double-wedge airfoil sections, had very nearly the
same drag coefficient at Mach number 0.9 as the wing-body combination
of the present test.

CONCLUSIONS

The results of flight measurements of zero-lift drag of an arrow wing with small body and of the body without the wing have been presented. Data obtained from a range of Mach numbers from 0.90 to 1.95 showed the following:

1. The force-break Mach number of the wing-body combination was 0.98. A maximum drag coefficient of 0.0125 occurred at Mach number 1.03. The drag coefficient decreased from the maximum value almost linearly to a value of 0.0096 at Mach number 1.95.

2. The wing with interference drag was approximately 70 percent of the drag of the wing-body model.

3. The zero-lift drag of the wing-body model was low throughout the Mach number range of the test.

Langley Aeronautical Laboratory
    National Advisory Committee for Aeronautics
   Langley Air Field, Va.

REFERENCES

1. Schult, Eugene D.: Comparison of Large-Scale Flight Measurements of Zero-Lift Drag at Mach Numbers from 0.9 to 1.7 of Two Wing-Body Combinations Having Similar 60° Triangular Wings with NACA 65A003 Sections. NACA RM L50I22, 1950.

2. Edwards, George G., and Stephenson, Jack D.: Tests of a Triangular Wing of Aspect Ratio 2 in the Ames 12-Foot Pressure Wind Tunnel. I - The Effect of Reynolds Number and Mach Number on the Aerodynamic Characteristics of the Wing with Flap Undeflected. NACA RM A7K05, 1947.

TABLE I

BODY AND WING AIRFOIL-SECTION ORDINATES

Airfoil section modified NACA 0004		Body ordinates	
Station (percent chord)	Upper and lower ordinates (percent chord)	Station (in. from nose)	Radius (in.)
0	0	0	0
1.25	.6325	1.000	.259
2.50	.8660	2.000	.491
5.00	1.1900	3.000	.703
7.50	1.4000	4.000	.893
10.00	1.5550	7.375	1.386
15.00	1.7780	10.375	1.654
20.00	1.9100	13.375	1.785
25.00	1.9780	15.375	1.808
30.00	2.0000	18.375	1.808
40.00	1.9310	20.000	1.806
Straight line	Straight line	23.000	1.787
75.00	1.0420	26.000	1.748
Straight line	Straight line	29.000	1.690
100.00	0	32.000	1.615
		35.000	1.526
		38.500	1.406
L.E. radius: 0.178		42.500	1.251
		46.500	1.082
		49.078	.965
		50.078	.909
		51.078	.837
		52.078	.742
		53.078	.618
		54.078	.457
		55.078	.253
		56.078	0
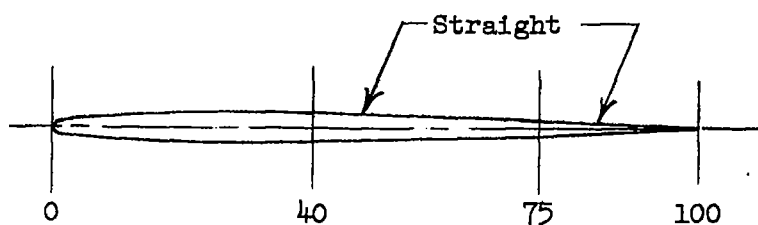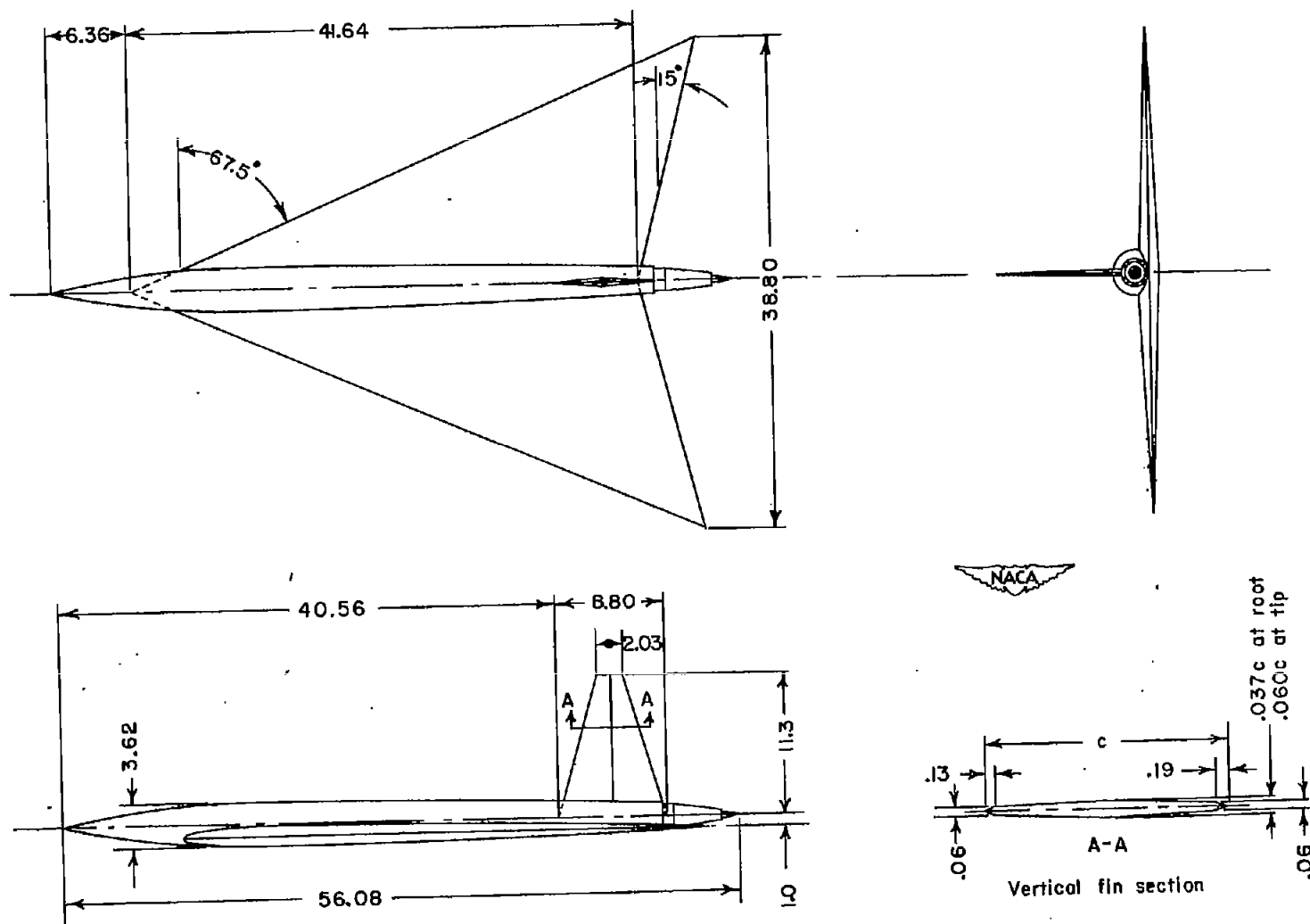
(a) Arrow wing-body combination.

Figure 1.- General arrangement of test models. All dimensions are in inches.

39.49

9.51

1.375

45°

16.27

B B

40.56

8.80

2.03

3.62

11.3

56.08

.045 R

.09

B-B
Horizontal fin section

.03 c

c

A-A
Vertical fin section

NACA
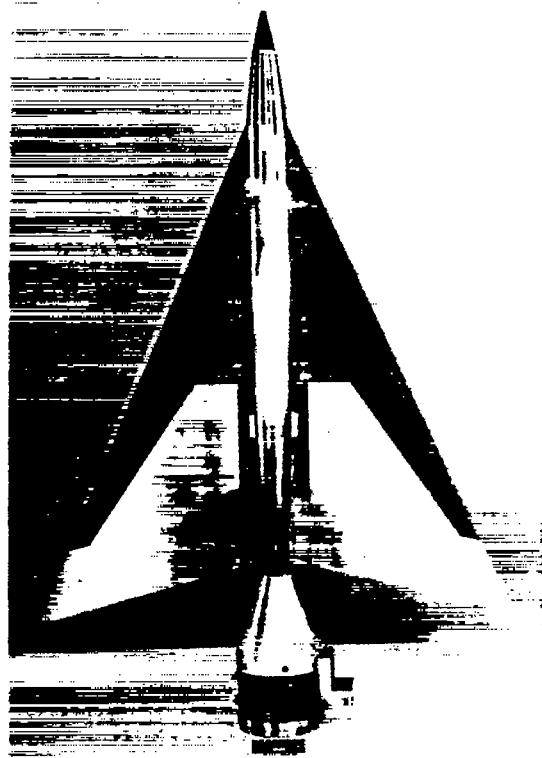
(b) Wingless model.
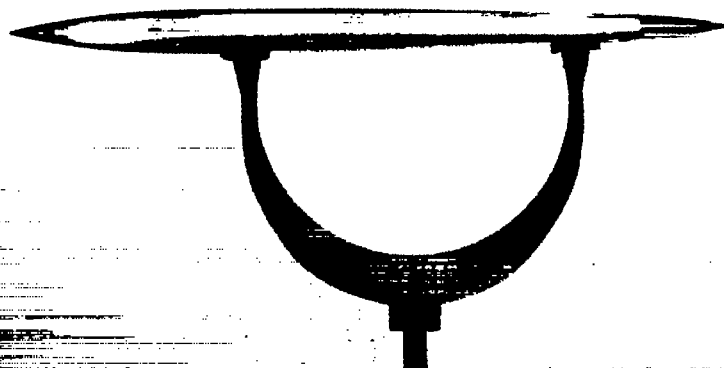
Figure 1.- Concluded.

(a) Side view.   L-65632

(b) Bottom view.   L-64659
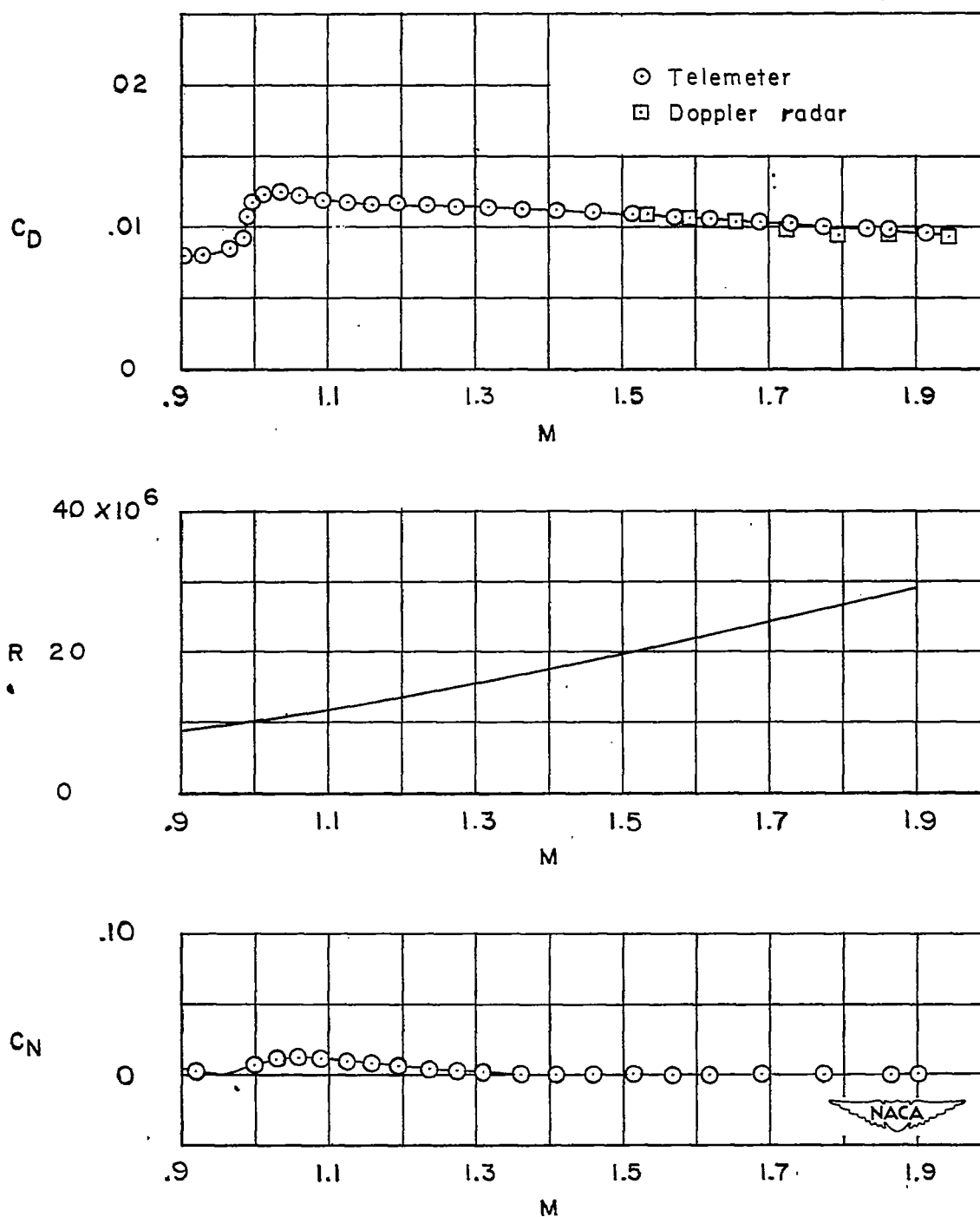
Figure 2.- Photographs of arrow wing-body model.
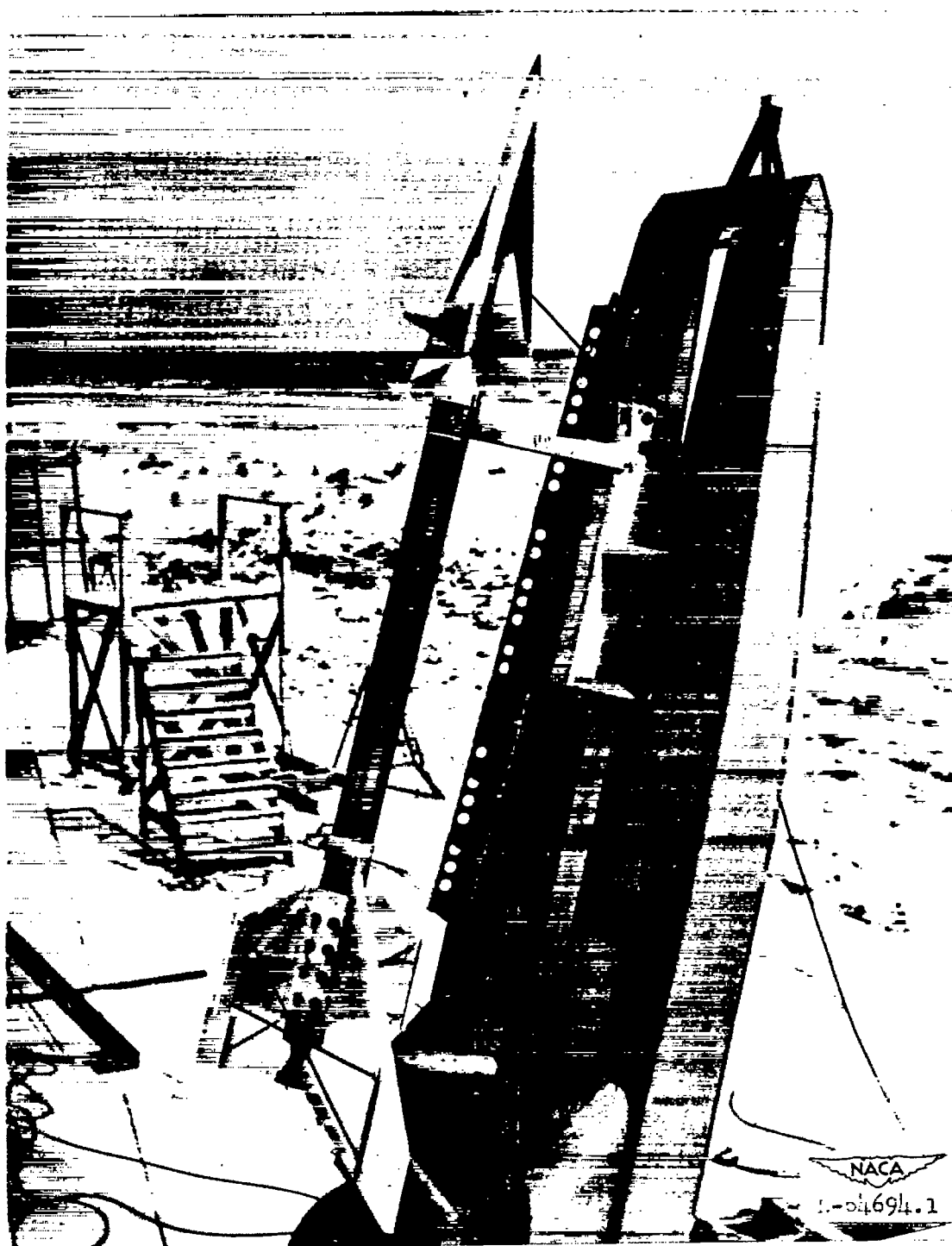
(a) Wing-body model and booster.

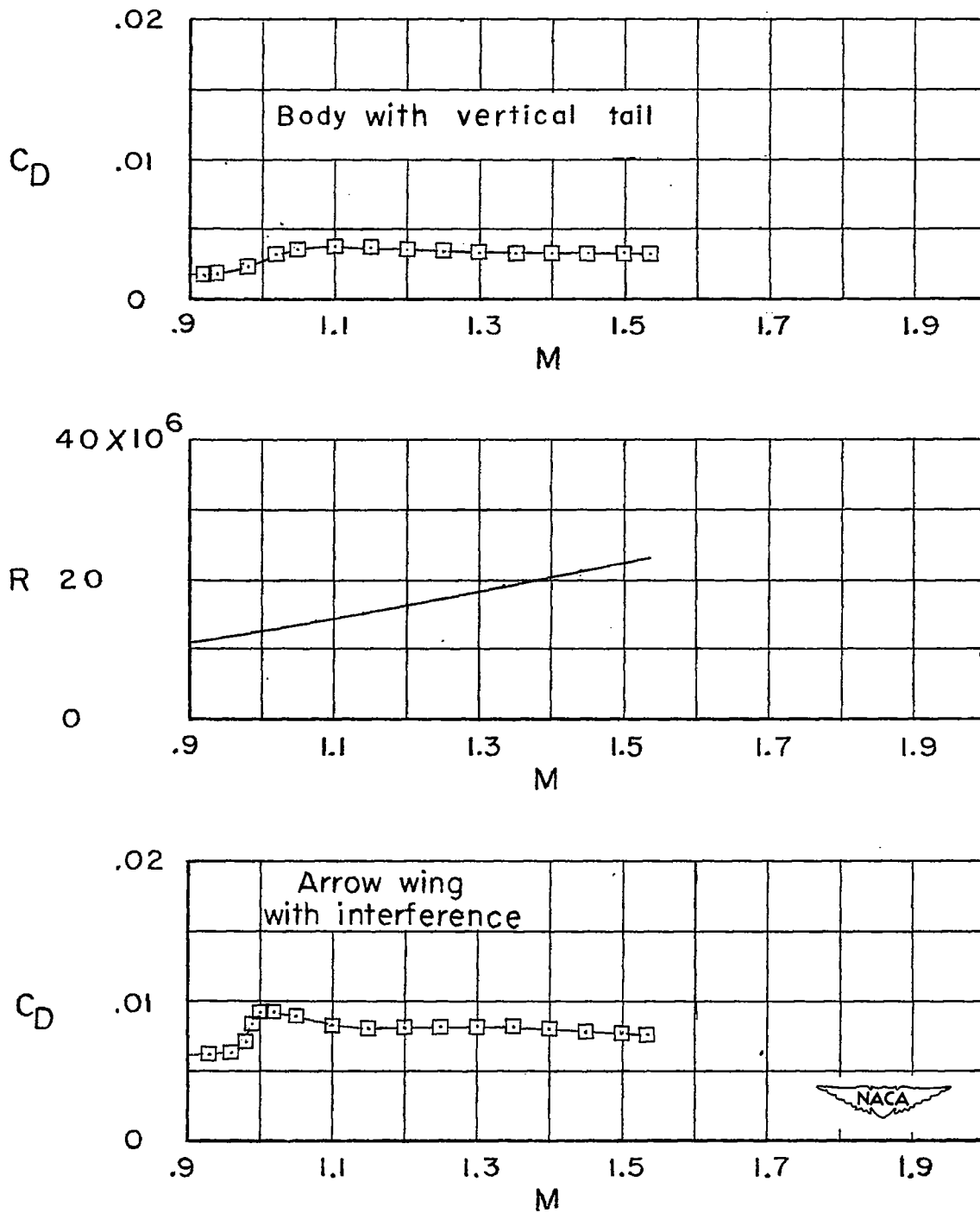Figure 3.- Model-booster combinations in launching attitude.

(b) Wingless model and booster.

Figure 3.- Concluded.

(a) C_D, R, and C_N against M for arrow wing-body model.

Figure 4.- Data from coasting flight of models.

(b) C_D and R against M from wingless model.
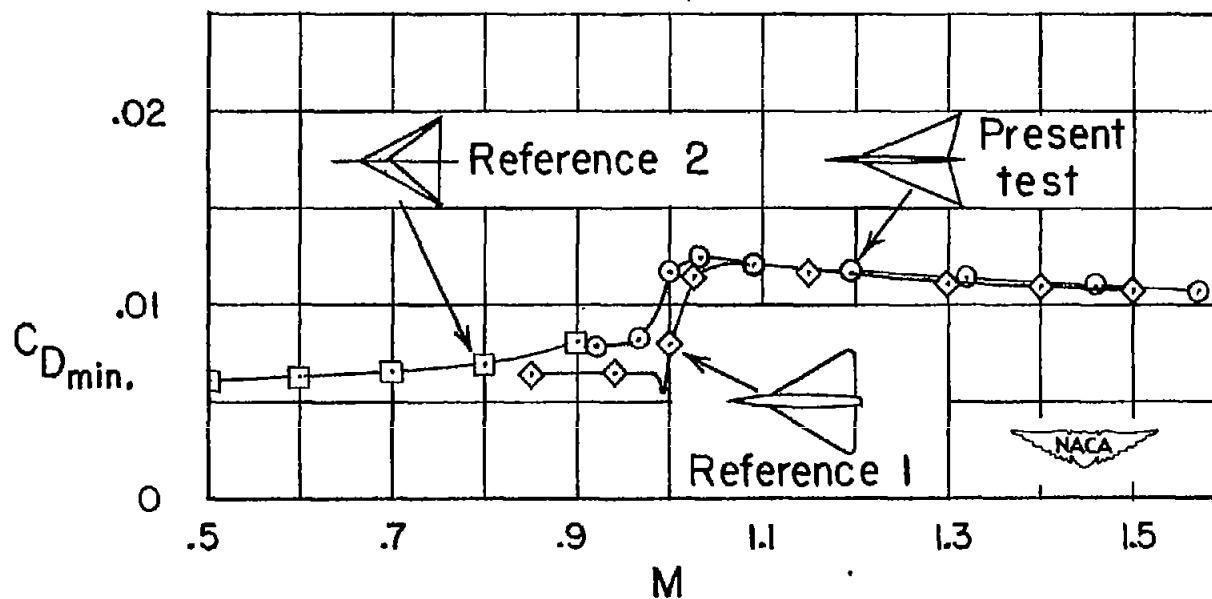
Figure 4.- Concluded.

Figure 5.- Variation of minimum drag coefficients of similar wing-body combinations at high Reynolds number with Mach number.